Massachusetts Institute of Technology

A Single Differential Equation for First-Excursion Time in a Class of Linear Systems

Matthew B. Greytak
Control Systems Engineer
Naval Surface Warfare Center, Carderock Division
Bethesda, Maryland 20817
Email: matthew.greytak@navy.mil

Franz S. Hover
Assistant Professor
Department of Mechanical Engineering
Massachusetts Institute of Technology
Cambridge, Massachusetts 02139
Email: hover@mit.edu

ABSTRACT

First-excursion times have been developed extensively in the literature for oscillators; one major application is structural dynamics of buildings. Using the fact that most closed-loop systems operate with a moderate to high damping ratio, we have derived a new procedure for calculating first-excursion times, for a class of linear continuous, time-varying systems. In several examples we show that the algorithm is both accurate and time-efficient. These are important attributes for real-time path planning in stochastic environments, and hence the work should be useful for autonomous robotic systems involving marine and air vehicles.

Nomenclature

$\mathbf{x}(t)$	State vector.
$y(t)$	System output, scalar.
$\mathbf{A}(t), \mathbf{G}(t), \mathbf{C}$	System matrices.
$\mathbf{w}(t)$	Unit Wiener noise process, vector.
$d_L(t), d_U(t)$	Lower and upper boundaries, scalar.
$\mathbf{\Sigma}(t)$	State covariance matrix.
$\Sigma_y(t)$	Output covariance, scalar.
$P_a(t)$	Probability of no collision, scalar.
$P_{hit}(t)$	Collision probability, $1 - P_a(t)$, scalar.

1 Introduction

The problem of predicting extreme deviations of response for a dynamic system subject to stochastic disturbances is well-known in the broad contexts of design, reliability theory, and Markov chains. In naval architecture, for example, both short- and long-term extremal loads are modeled and employed extensively through all stages of offshore system design and

operation, including fatigue analysis. Calculations of the highest average 1/n'th response amplitude are perhaps the most common in applications. Another quantity of major interest in stochastic dynamics is the cumulative probability of exceeding a given threshold level $d(t)$ on the system output y before time T: $P(T) = P(\exists t \in [t_o, T] \mid y(t) > d(t))$. In Markov chains, this boundary delineates transient and absorbing states. In reliability theory, this problem is known as the first-excursion time; the reliability function is $R(T) = 1 - P(T)$.

The analysis of such problems has a long and rich history, both in the physics and engineering communities. Particle absorption is the simplest scenario, characterizing the distribution of a population of particles as they move at constant speed near a parallel boundary, while diffusing in the lateral direction. Particle absorption focuses mainly on random walks, however, a canonical case that does not necessarily extend to more general linear systems [1–4]. Seminal work by Crandall and others [5–7] explored the statistics of first-excursion for a lightly-damped oscillator with Gaussian process noise. Accurate formulas have been vigorously pursued especially for lightly damped oscillators, because a low damping ratio corresponds with long impulse responses, leading to a very long correlation time which complicates the analysis. The LTI oscillator with stationary noise in fact admits an eigenvalue solution [8], where the eigenvectors are confluent hypergeometric functions. For more complicated linear dynamical systems, approaches vary; He, for example, recently calculated moments of the first-excursion time distribution, and combined these with a fitted expression for the decay constant α [9]; Au and Beck employed an importance sampling approach with very high accuracy [10]. The main application in these two works is the response of buildings to earthquakes, and here the stochastic excitation usually appears through a time-varying modulation function $G(t)$. The most general problems, including those with nonlinearities, are addressed through stochastic averaging [8].

Another type of first-excursion problem arises for mobile and robotic systems that must plan and execute a path with bounded deviations [11, 12]; formal treatment of this problem in the robotics community is known as chance-constrained planning, generally posed in discrete time. Typical disturbances include wind in aeronautical applications, and wind, waves, and currents in marine applications. The bad effects of these disturbances are often exacerbated by the desire to perform precision tasks, such as inspection or intervention; it may not be only contact with a physical boundary that is problematic, but rather that a sensor is out of range [13]. Further, deviations from a designed path could jeopardize the fidelity of communication links or navigation information. Uncertainties in the dynamic behavior of a vehicle motivate conservative paths through obstacles, wherein avoiding collision is valued highly relative to a minimum-time or minimum-distance plan. This tradeoff generates a natural optimization problem, captured in the simple cost function $J = T_f/(1 - P(T_f))$, where T_f is the time to execute the maneuver, and $P(T_f)$ is the probability of hitting an obstacle along the way, as used in [14]. Absent of any free parameters, this cost function amplifies the time cost approximately by the number of trials required to achieve a zero-collision transit.

Toward this end, the present paper gives, for the first time to our knowledge, a single ordinary differential equation (SDE) that governs the first excursion time probability for a single output channel. The approach applies to any second-order or higher linear system with no direct feed-through of the noise. That is, if $\dot{\mathbf{x}} = \mathbf{A}\mathbf{x} + \mathbf{G}\mathbf{w}$, $y = \mathbf{C}\mathbf{x}$ are the system equations with noise $\mathbf{w}$, then we require $\mathbf{CG} = 0$. The development hinges also on a key assumption that the surviving trajectories are
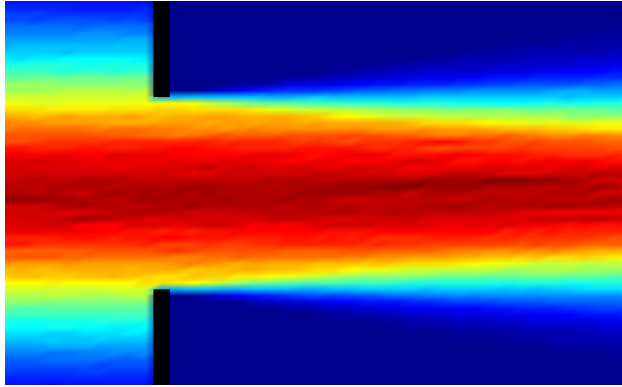
Fig. 1. The pdf of the output of a dynamic system diffuses past a "gate," an instantaneous constraint. Our complete solution is the limiting case as the distance between consecutive gates approaches zero.

well-approximated by a truncated, zero-mean normal distribution. This makes our SDE solution quite poor at lower damping ratios, $\zeta < 0.2$, say. On the other hand, controlled dynamic systems typically have higher damping in the closed loop.

There are several advantages to writing the the reliability evolution in a differential equation. First, we seamlessly accommodate time variations in the plant matrix $\mathbf{A}(t)$, the noise gain matrix $\mathbf{G}(t)$, and the boundaries $d_L(t)$ and $d_U(t)$. Second, as we show in our examples, the SDE solution can sometimes be computed in a time that is competitive with that of a *single* Monte Carlo trial; computation speed is critical for autonomous mobile robots, where paths are commonly evaluated in real-time, during operations. Finally, the new scheme should lend itself well to additional uncertainty analysis, because it places the white noise aspect of the stochastic response into a deterministic framework. This can then be further decomposed to characterize the effects of parametric uncertainty, for example through probabilistic collocation [15]. This last topic is outside our present scope.

The paper outline is as follows. We give a concise statement of our formulas, with two short examples to illustrate the closeness of the approximations relative to Monte Carlo trials, and to indicate typical computational costs. The derivation is then given, in which we evolve trajectories after passing a single instantaneous gate, as shown in Fig. 1, combine multiple gate passages, and finally let the spacing of the gates approach zero to approximate a smooth boundary.

2 Problem Statement and Solution

2.1 System Model

The state vector $\mathbf{x} \in \mathcal{R}^q$ evolves through time according to the stochastic differential equation $\delta\mathbf{x} = \mathbf{A}\mathbf{x}\delta t + \mathbf{G}\delta\mathbf{w}$, where $\mathbf{w}$ is a Wiener process of unit magnitude: $\mathbf{w}(t) \sim N(\mathbf{0}, \mathbf{I}t)$ and $\delta\mathbf{w} \sim N(\mathbf{0}, \mathbf{I}\delta t)$. The class of problems we address allows both $\mathbf{A}$ and $\mathbf{G}$ to be time-varying; we will not show the dependence on time except where necessary for clarification. We are interested in a scalar output defined by $y = \mathbf{C}\mathbf{x}$, and we assume that $\mathbf{C}\mathbf{G} = 0$, that is, the process noise acts through the dynamics and not on the output directly. In the absence of any boundaries, the state variance $\mathbf{\Sigma} = E[\mathbf{x}\mathbf{x}^T]$ evolves according to the Riccati equation $\dot{\mathbf{\Sigma}} = \mathbf{A}\mathbf{\Sigma} + \mathbf{\Sigma}\mathbf{A}^T + \mathbf{G}\mathbf{G}^T$, and the variance of the unconstrained output is $\Sigma_y = \mathbf{C}\mathbf{\Sigma}\mathbf{C}^T$. The absorbing boundaries are given by lower and upper constraints, d_L and d_U respectively, which can be time-varying functions with

discontinuities.

2.2 Solution Summary

The probability that the particle has not violated a constraint after t seconds is $P_a(t)$, and it evolves according to the differential equation $\dot{P}_a(t) = -C(t)P_a(t)$, with the initial condition $P_a(0) = 1$. $P_a(t)$ is called the reliability function. The collision probability is $P_{hit}(t) = 1 - P_a(t)$; it is the cumulative distribution function for the first excursion time. The decay constant C is a specific function as follows:

$$
\begin{aligned}
C \ &= \ C_1 + C_2 + C_3 + C_4, \ \text{ where} \\
C_1 &= \ \ (\dot{d}_L/n) \times N(d_L \ : 0, \Sigma_y) \times E_2(h_L : 0, \Sigma_c) \\
C_2 &= -(\dot{d}_U/n) \times N(d_U : 0, \Sigma_y) \times E_1(h_U : 0, \Sigma_c) \\
C_3 &= (1/n) \times N(d_L : 0, \Sigma_y) \\
&\qquad \times (\Sigma_c N(h_L \ : 0, \Sigma_c) - h_L E_2(h_L : 0, \Sigma_c)) \\
C_4 &= (1/n) \times N(d_U : 0, \Sigma_y) \\
&\qquad \times (\Sigma_c N(h_U : 0, \Sigma_c) + h_U E_1(h_U : 0, \Sigma_c)).
\end{aligned}
\tag{1}
$$

The functions $N()$, $E_1()$ and $E_2()$ represent the probability density function (pdf) of a normally-distributed random variable, its cumulative distribution, and the complement of the cumulative distribution, respectively:

$$
N(x : a, A) = \frac{1}{\sqrt{2\pi A}} \exp\left(-\frac{(x-a)^2}{2A}\right)
\tag{2}
$$

$$
E_1(x : a, A) = \frac{1}{2}\left(1 + \text{erf}\,\frac{x-a}{\sqrt{2A}}\right) = \int_{-\infty}^{x} N(x : a, A)dx
\tag{3}
$$

$$
E_2(x : a, A) = \frac{1}{2}\left(1 - \text{erf}\,\frac{x-a}{\sqrt{2A}}\right) = \int_{x}^{\infty} N(x : a, A)dx
\tag{4}
$$

$$
= 1 - E_1.
$$

We denote by n the probability that instantaneously $d_L < y < d_U$:

$$
n = P(d_L < y < d_U) = \frac{1}{2}\left(\text{erf}\,\frac{d_U}{\sqrt{2\Sigma_y}} - \text{erf}\,\frac{d_L}{\sqrt{2\Sigma_y}}\right),
\tag{5}
$$

and the remaining quantities in Eqn. (1) are:

$$\Sigma_y = \mathbf{C\Sigma C}^T \tag{6}$$

$$\Sigma_c = \mathbf{CA\Sigma A}^T\mathbf{C}^T - (\mathbf{C\Sigma A}^T\mathbf{C}^T)^2 / \Sigma_y \tag{7}$$

$$h_L = d_L \times \mathbf{C\Sigma A}^T\mathbf{C}^T / \Sigma_y \tag{8}$$

$$h_U = d_U \times \mathbf{C\Sigma A}^T\mathbf{C}^T / \Sigma_y. \tag{9}$$

The solution requires us to evolve Σ and P_a as functions of time. Σ contains the natural dynamic behavior of the unconstrained ensemble and does not depend on the boundaries; the differential equation for P_a uses Σ, and accounts for the boundaries.

2.3   Example 1: Time-Varying Constraints

We consider the fourth-order system given by the following matrices:

$$\mathbf{A} = \begin{bmatrix} -0.175 & 0.125 & 0.05 & 0.1 \\ -0.390 & -0.690 & -0.156 & -0.312 \\ 1 & 0 & 0 & 0.25 \\ 0 & 1 & 0 & 0 \end{bmatrix}, \tag{10}$$

$$\mathbf{G} = \begin{bmatrix} \sqrt{0.001} & 0 \\ 0 & \sqrt{0.001} \\ 0 & 0 \\ 0 & 0 \end{bmatrix}, \qquad \mathbf{C} = \begin{bmatrix} 0 & 0 & 1 & 0 \end{bmatrix}.$$

This represents a holonomic marine vehicle [14] following a straight reference path under closed-loop control, with $\mathbf{x} = [v, r, y, \psi]^T$, where v is sway velocity, r is yaw rate, y is cross-track position error, and ψ is heading. This plant has four poles; two are real and the others have a damping ratio of 0.412. The vessel moves between two non-straight walls defined by,

$$d_L(t) = -0.55 + 0.03 \sin\left(2\pi t/25\right),$$
$$d_U(t) = 0.60 - 0.05 \sin\left(2\pi t/40\right). \tag{11}$$

We ran Monte Carlo simulation with 50,000 trials, starting from zero initial conditions; one hundred example trajectories
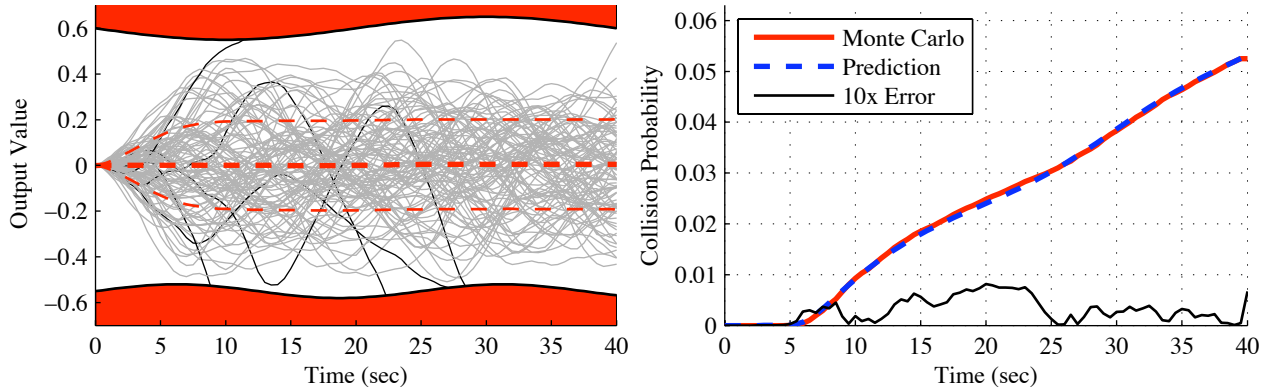
Fig. 2. The system shown in Eqn. (10) with two time-varying constraints, Eqn. (11). The first plot shows one hundred trajectories from a 50,000-point Monte Carlo simulation. The trajectories drawn in black violate one of the constraints, while the gray trajectories do not. The red curves show the mean and standard deviation of the Monte Carlo simulation. The second plot shows the particle absorption fraction P_{hit} as given by the SDE estimate (blue dashed) and the Monte Carlo estimate (red). The error between these is shown in black.

are shown in Fig. 2, along with the SDE and MC collision probability estimates. We can see that the SDE is correctly modulating the collision probability as the boundaries vary. The MC trials result in a standard error on $P_{hit}(t = 40)$ of less than 0.001, and this value is close to the discrepancy between the two estimates. Hence the precision of the solution would be adequate for path planning with confidence levels above 99%, at least over this time scale. In longer runs, we expect growing errors because of our assumption of truncated normal distributions.

2.4 Example 2: Time-Varying Plant

We consider a second-order time-varying system,

$$\ddot{y} + b/m(t)\dot{y} + k/m(t)y = fw, \tag{12}$$

with $m(t) = 120 - 0.9t$, $b = 10$, $k = 1$, and $f = 0.0125$. This can serve as a simple model for the lateral dynamics of a rocket that is consuming fuel while subject to acceleration disturbances. The damping ratio of the system is initially 0.456 but it increases to 0.913 by 100 seconds. The boundaries are straight and fixed at ± 0.50 units. Figure 3 shows the results of a 50,000-point Monte Carlo simulation, along with the SDE estimate. The standard error of the MC estimate is about 0.001 again, and we have excellent agreement with the prediction.

2.5 Computational Cost

Our approach has attractive computational cost; fast evaluation of the excursion probabilities is important for on-line planning schemes in mobile autonomous agents. As a cost reference, Au and Beck [10] achieved good accuracy for a lightly-damped (2%) oscillator through importance sampling, with about ten trials. Each such trial involves the solution of a q-state ordinary differential equation, with a discretization of time to handle noise. In contrast, our method solves the matrix Riccati equation, with $q(q - 1)/2$ states, and the one-state ODE described in Eqn. (1). With no explicit sampling of noise, these
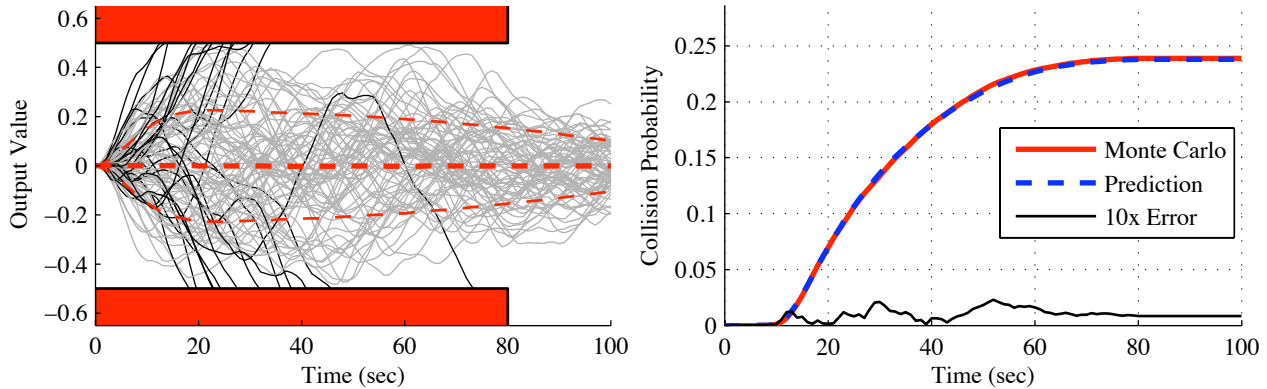
Fig. 3. A time-varying second-order system, Eqn. (12), representing the lateral dynamics of a rocket. The first plot shows one hundred trajectories from a 50,000-point Monte Carlo simulation. The second plot shows the particle absorption fraction P_{hit} as given by the SDE estimate (blue dashed) and the Monte Carlo estimate (red). The error between these is shown in black.

can be handled in continuous time, and we use an adaptive step-size Runge-Kutta routine. In our MC trials we discretize time to inject noise with a zero-order hold, but employ the same Runge-Kutta solver for the system dynamic response in the intervals, for consistency. The integration tolerance settings for the MC and the SDE calculations are identical.

Relative computation times for each example above are listed in Tab.1. The SDE time, which includes the Riccati equation component, is comparable to or better than a single MC trial in both cases. This likely occurs because the MC simulation has discontinuities in the noise, requiring vigorous adjustments of the step-size to maintain accuracy, whereas the SDE is a completely continuous-time formulation. More broadly, the relative cost of the SDE solution will depend on the specific application, with factors including the system size, the spectral content of $\mathbf{A}$, the output matrix $\mathbf{C}$, and the time variations of A, G, d_L, and d_U. Other factors are the choice and extent of the noise discretization.

Table 1. Computation times

Example	MC Noise Time Step	MC Cost (avg.)	SDE Cost
1	0.2	0.469	0.273
2	1.0	0.370	0.362

2.6 Remarks

1. As noted, the formulas hold for time-varying $\mathbf{A}$, $\mathbf{G}$, d_L and d_U. The constraints d_L and d_U are assumed to be continuous, except for two special cases. In Example 2, the constraint is removed entirely at $t = 80$ seconds and here $\dot{P}_a$ is set explicitly to zero, as there are no further losses. In general, if one of the constraints is removed then C_1 and C_3, or C_2 and C_4, as appropriate, are set to zero. The other special case is activating the constraint instantaneously, as shown in Fig. 1. The initial condition for the $P_a(t)$ differential equation is $n(t_0)$; this works for single-sided and double-sided constraints. Single-sided constraints are handled cleanly by setting $d_L(t) = -\infty$ or $d_U(t) = \infty$.

2. We reiterate an important assumption in our work: that the pdf of the surviving population is always a zero-mean Gaussian that is truncated, perhaps asymmetrically. This is known to be inaccurate when a low damping ratio affects y, as in the classical first excursion time problem for oscillators. For example, in Langley's [7] Tab. 2, the mean first excursion time clearly is a function of both the damping ratio and the nondimensional threshold level. Inspection shows that our formulas do not preserve this dependence on damping ratio, and this deficiency is significant for damping ratios less than about 0.2. We emphasize also that our formulation pertains to a scalar output only, and this distinguishes it from more complicated and intensive problems in which one desires to track a multi-channel output relative to a feasible set.

3 Derivation

We first compute how the output distribution expands in a small time step after an instantaneous "gate" is encountered, and then consider the limit as the time step goes to zero. A number of variables used in the derivation are listed in Tab. 2. Σ_y represents the unconstrained variance of the output at t, while $\Sigma_{\dot{y}}$ is the variance of the instantaneous change in y and Σ_ρ represents the correlation between y and $\dot{y}$. Σ_γ represents the variance of the output as it diffuses from t to $t + \Delta t$. Note that Σ_γ is a function of the small time increment Δt. The other variables in the table are defined for convenience in the derivation. This derivation makes extensive use of the notation in Eqns. (2-4).

Table 2. Variables used in the derivation of $C(t)$

$$
\begin{aligned}
\mathbf{\Sigma} &= E[\mathbf{x}\mathbf{x}(t)^T] \\
\Sigma_y &= \mathbf{C\Sigma C}^T \\
\Sigma_{\dot{y}} &= \mathbf{CA\Sigma A}^T\mathbf{C}^T \\
\Sigma_\rho &= \mathbf{C\Sigma A}^T\mathbf{C}^T \\
\rho &= \Sigma_\rho / \sqrt{\Sigma_y \Sigma_{\dot{y}}} \\
\Sigma_{y\rho} &= \Sigma_y \left(1 - \rho^2\right) \\
\Sigma_\gamma &= \Sigma_y + 2\Sigma_\rho \Delta t + \Sigma_{\dot{y}} \Delta t^2 \\
\Sigma_c &= \Sigma_{\dot{y}} - \Sigma_\rho{}^2/\Sigma_y
\end{aligned}
$$

3.1 First Constraint Encounter

The pdf of the output y in the absence of boundaries is given by $p(y)_{open} = N(y:0,\Sigma_y)$. Let us consider a constraint that is active at an instant; the pdf of the surviving population is rescaled so that the integral is unity:

$$
p(y) = \begin{cases} N(y:0,\Sigma_y)/n \text{ for } d_L < y < d_U, \\ 0 \qquad\qquad \text{otherwise,} \end{cases}
\tag{13}
$$

where n is defined in Eqn. (5).

We are interested next in how the pdf of successful particles evolves a short time after passing an instantaneous gate, as

shown in Fig. 1. Again for the condition of no constraints, the joint probability density function of y and its derivative is, defining $\mathbf{z} = [y, \dot{y}]^T$,

$$
\begin{aligned}
p(\mathbf{z})_{open} &= \frac{1}{2\pi\sqrt{|\mathbf{\Sigma}_z|}}\exp\left(-\frac{1}{2}\mathbf{z}^T\mathbf{\Sigma}_z^{-1}\mathbf{z}\right) \\
&= N(y:0,\Sigma_y) \\
&\quad \times N\left(\dot{y}:y\rho\sqrt{\Sigma_{\dot{y}}/\Sigma_y},\ \Sigma_{\dot{y}}(1-\rho^2)\right),
\end{aligned}
\tag{14}
$$

where $\mathbf{\Sigma}_z = [\Sigma_y\ \Sigma_\rho;\ \Sigma_\rho\ \Sigma_{\dot{y}}]$. The second equation is obtained by completing the square. For a small time step Δt, it follows directly that

$$
\begin{aligned}
p(y,\Delta y)_{open} &\approx N(y:0,\Sigma_y) \\
&\quad \times N\left(\Delta y:y\rho\Delta t\sqrt{\Sigma_{\dot{y}}/\Sigma_y},\ \Sigma_{\dot{y}}(1-\rho^2)\Delta t^2\right)\Delta t,
\end{aligned}
\tag{15}
$$

and $p(y,\Delta y) = p(y,\Delta y)_{open}/n$ over the domain of interest, as above. Now let $\gamma \equiv y + \Delta y$, the particle location a time Δt after passing the gate defined by $d_L(t)$ and $d_U(t)$. To evaluate the pdf for γ we first compute the cumulative probability $P(\gamma < c)$. Integrating $p(y,\Delta y)$ over the whole domain is equivalent to integrating $p(y,\Delta y)_{open}/n$ along $d_L < y < d_U$. The latter approach is simpler, and this smaller domain of integration is shown in Fig. 4. The resulting integrals are shown below.

$$
\begin{aligned}
P(\gamma < c) &= \int_{-\infty}^{c-d_U}\int_{d_L}^{d_U} p(y,\Delta y)_{open}/n\, dy\, d\Delta y \\
&\quad + \int_{c-d_U}^{c-d_L}\int_{d_L}^{c-\Delta y} p(y,\Delta y)_{open}/n\, dy\, d\Delta y
\end{aligned}
\tag{16}
$$

Employing the fact that the inner integrals can be written in terms of the error function, using the fundamental theorem of calculus[1] to differentiate $P(\gamma < c)$ with respect to c, and exploiting the fact that the product of two Gaussians is proportional

---

[1] The fundamental theorem of calculus as used here is:

$$
\text{If} \qquad F(x) = \int_{a(x)}^{b(x)} f(x,z)dz
$$

$$
\text{then} \quad \frac{d}{dx}F(x) = f(x,b(x))\frac{db}{dx} - f(x,a(x))\frac{da}{dx} + \int_{a(x)}^{b(x)}\frac{\partial}{\partial x}f(x,z)dz
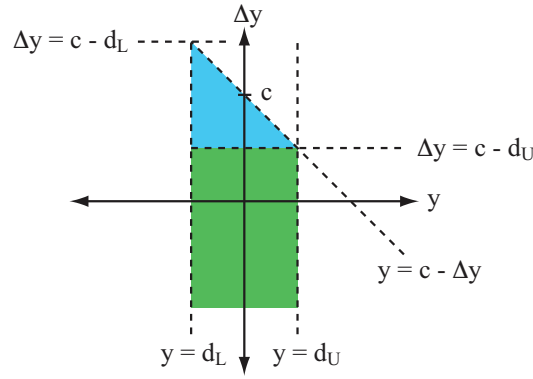$$

Fig. 4. The domain of integration for $P(\gamma < c)$ Eqn. (16), bounded by $d_L < y < d_L$ and $\Delta y < c - y$. The first term is represented by the shaded triangle and the second term is represented by the open rectangle.

to another Gaussian[2], after some manipulation we arrive at the pdf of γ, to first order in Δt:

$$
p(\gamma) = \frac{1}{2n}N(\gamma:0,\Sigma_\gamma) \times \left(\text{erf } \frac{\gamma(\Sigma_y + \Sigma_\rho \Delta t)/\Sigma_\gamma - d_L}{\Delta t \sqrt{2\Sigma_c \Sigma_y/\Sigma_\gamma}} \right.
$$
$$
\left. - \text{erf } \frac{\gamma(\Sigma_y + \Sigma_\rho \Delta t)/\Sigma_\gamma - d_U}{\Delta t \sqrt{2\Sigma_c \Sigma_y/\Sigma_\gamma}} \right). \tag{17}
$$

This pdf for γ is plotted in Fig. 5 for the first example system, with $\Delta t = 0.2$, 0.5, and 1.0 seconds after passing the gate. The pdf is compared to Monte Carlo simulations having 100,000 trajectories, validating the formula. The accuracy of the predicted pdf decreases as Δt increases, in accordance with our approximations.

3.2 Wall Diffusion

We consider the limit of $\Delta t \to 0$. Note that $\gamma - d_U$ and $\gamma - d_L$ in the numerator of Eqn. (17) are functions of Δt. The probability of survival a time Δt after the gate (modeled as a second gate at $t + \Delta t$) is:

$$
P_a(t + \Delta t) = P_a(t) \times P\left(d_L(t + \Delta t) < \gamma < d_U(t + \Delta t)\right) \tag{18}
$$

---

[2]If $N(a,A)$ and $N(b,B)$ are normal distributions with means a and b and variances A and B, respectively, then the product of the two distributions is:

$$
N(a,A) \times N(b,B) = \frac{1}{2\pi\sqrt{AB}} \exp\left(-\frac{\left(x - \frac{Ba+Ab}{A+B}\right)^2}{2\frac{AB}{A+B}}\right) \times \exp\left(-\frac{(a-b)^2}{2(A+B)}\right)
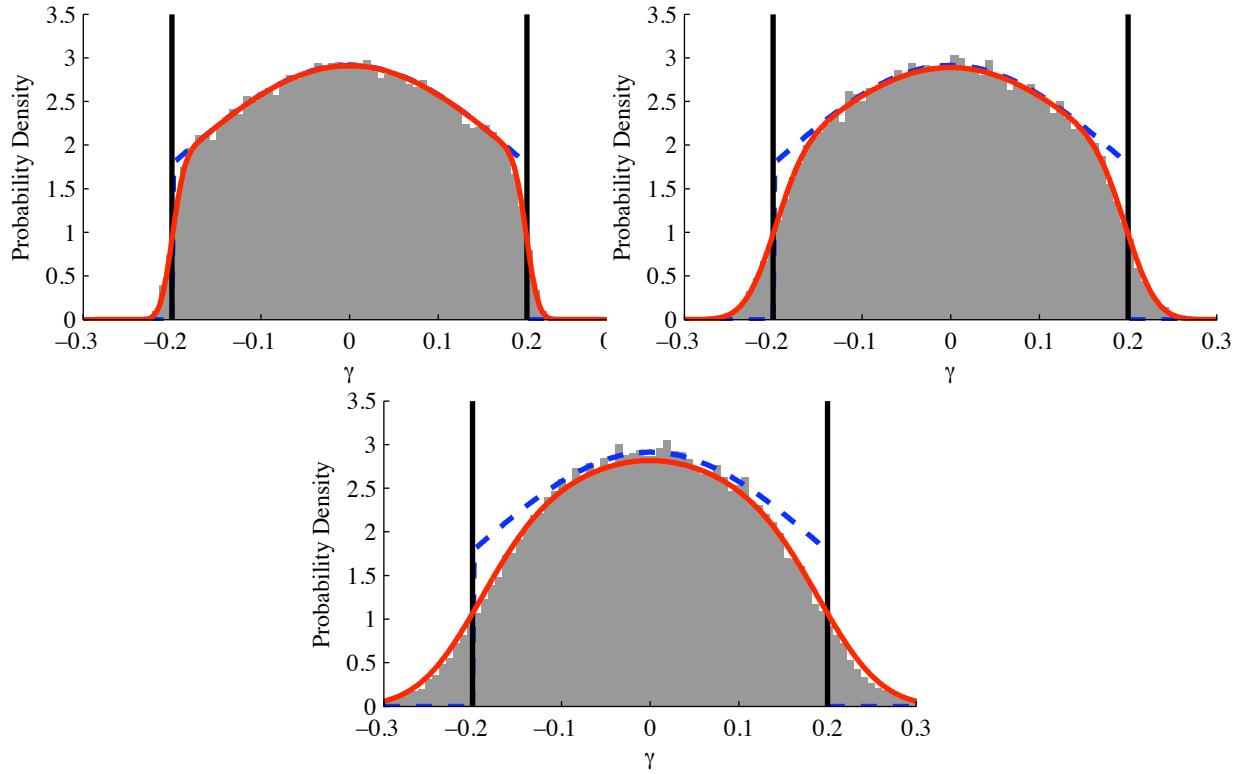$$

Fig. 5. $p(\gamma)$ after Δt = 0.2, 0.5, and 1.0 seconds with the system in Example 1 and walls at $d = \pm 0.2$. The result is validated with the histogram from a 100,000-point Monte Carlo simulation (gray bars). The pdf at t_0, $p(y)$, is the dashed blue line.

so that

$$
\begin{aligned}
\dot{P}_a &= \lim_{\Delta t \to 0} \frac{P_a(t + \Delta t) - P_a(t)}{\Delta t} \\
&= P_a \lim_{\Delta t \to 0} \frac{P(d_L(t + \Delta t) < \gamma < d_U(t + \Delta t)) - 1}{\Delta t} \\
&= -P_a \lim_{\Delta t \to 0} \frac{P(\gamma \leq d_L(t + \Delta t) \text{ or } \gamma \geq d_U(t + \Delta t))}{\Delta t} \\
&\equiv -C P_a.
\end{aligned}
\tag{19}
$$

Define $F(t) = P(\gamma \leq d_L(t + \Delta t) \text{ or } \gamma \geq d_U(t + \Delta t))$, so that

$$
C = \frac{dF}{dt} = \frac{d}{dt} \left[\int_{-\infty}^{d_L(t + \Delta t)} p(\gamma) d\gamma + \int_{d_U(t + \Delta t)}^{\infty} p(\gamma) d\gamma \right].
\tag{20}
$$

This can be expanded using the fundamental theorem of calculus, leading to

$$
\begin{aligned}
C &= \dot{d}_L\, p(d_L) - \dot{d}_U\, p(d_U) \\
&+ \int_{-\infty}^{d_L(t+\Delta t)} \frac{d}{dt} p(\gamma)d\gamma + \int_{d_U(t+\Delta t)}^{\infty} \frac{d}{dt} p(\gamma)d\gamma \\
&\equiv C_1 + C_2 + C_3 + C_4.
\end{aligned}
\tag{21}
$$

3.2.1 C_1 and C_2: Changing Wall Distance, Constant PDF

C_1 represents the effect of a changing lower wall distance. The first term of the numerator of Eqn. (17) can be simplified as follows, keeping the leading terms as appropriate:

$$
\begin{aligned}
\gamma(\Sigma_y + \Sigma_\rho \Delta t)/\Sigma_\gamma &\approx d_L(\Sigma_y + \Sigma_\rho \Delta t)/\Sigma_\gamma \\
&= d_L(\Sigma_\gamma - 2\Sigma_\rho \Delta t - \Sigma_{\dot{y}}\Delta t^2 + \Sigma_\rho \Delta t)/\Sigma_\gamma \\
&\approx d_L(\Sigma_\gamma - \Sigma_\rho \Delta t)/\Sigma_\gamma \\
&\approx d_L(1 - \Sigma_\rho \Delta t/\Sigma_y)
\end{aligned}
\tag{22}
$$

With this approximation, C_1 is:

$$
\begin{aligned}
C_1 &= \frac{\dot{d}_L}{2n}\, N(d_L : 0, \Sigma_y) \\
&\times \left(\operatorname{erf} \frac{d_L\left(1 - \Sigma_\rho \Delta t/\Sigma_y\right) - d_L}{\Delta t \sqrt{2\Sigma_c}} - \operatorname{erf} \frac{d_L - d_U}{\Delta t \sqrt{2\Sigma_c}} \right).
\end{aligned}
\tag{23}
$$

The numerator of the first error function can be written as $-h_L\Delta t$ whre $h_L \equiv d_L\Sigma_\rho/\Sigma_y$. Next, because $d_U > d_L$, the second error function always evaluates to -1 when $\Delta t \to 0$. These quantities are inserted into Eqn. (23), yielding

$$
\begin{aligned}
C_1 &= \frac{\dot{d}_L}{2n}\, N(d_L : 0, \Sigma_y) \left(\operatorname{erf} \frac{-h_L}{\sqrt{2\Sigma_c}} + 1 \right) \\
&= \frac{\dot{d}_L}{n}\, N(d_L : 0, \Sigma_y) \times E_2\left(h_L : 0, \Sigma_c\right).
\end{aligned}
\tag{24}
$$

C_2 is easily derived through a parallel derivation, with d_U and h_U replacing d_L and h_L, respectively.

3.2.2 C_3 and C_4: Constant Wall Distance, Diffusing PDF

The chain rule gives

$$
\begin{aligned}
C_3 = &\int_{-\infty}^{d_L} \frac{1}{2n} \frac{d}{dt} N(\gamma : 0, \Sigma_\gamma) \times \left(\text{erf} \frac{\gamma \left(1 - \Sigma_\rho \Delta t / \Sigma_y \right) - d_L}{\Delta t \sqrt{2\Sigma_c}} \right. \\
&\left. - \text{erf} \frac{\gamma \left(1 - \Sigma_\rho \Delta t / \Sigma_y \right) - d_U}{\Delta t \sqrt{2\Sigma_c}} \right) d\gamma \\
&+ \int_{-\infty}^{d_L} \frac{1}{2n} N(\gamma : 0, \Sigma_\gamma) \times \frac{d}{dt} \left(\text{erf} \frac{\gamma \left(1 - \Sigma_\rho \Delta t / \Sigma_y \right) - d_L}{\Delta t \sqrt{2\Sigma_c}} \right. \\
&\left. - \text{erf} \frac{\gamma \left(1 - \Sigma_\rho \Delta t / \Sigma_y \right) - d_U}{\Delta t \sqrt{2\Sigma_c}} \right) d\gamma \\
\equiv & \; C_{3a} + C_{3b}.
\end{aligned}
\tag{25}
$$

In C_{3a}, the first part of the integrand is nonzero and finite as $\Delta t \to 0$. Meanwhile, the first error function is -1 when $\gamma < d_L$ and zero when $\gamma = d_L$; the second error function is -1 everywhere since $\gamma \le d_L < d_U$. Thus the integrand of C_{3a} is only nonzero and finite at a single point, $\gamma = d_L$, and zero everywhere else, so that $C_{3a} = 0$.

We turn to the second integral, C_{3b}, and shift the limits of integration by introducing a new variable $\gamma_L \equiv \gamma - d_L$, which scales with Δt. The chain rule provides the expansion

$$
\begin{aligned}
C_{3b} = &\int_{-\infty}^{0} \frac{1}{2n} N(\gamma_L + d_L : 0, \Sigma_\gamma) \\
&\times \frac{d}{dt} \left(\text{erf} \frac{(\gamma_L + d_L)\left(1 - \Sigma_\rho \Delta t / \Sigma_y\right) - d_L}{\Delta t \sqrt{2\Sigma_c}} \right. \\
&\left. - \text{erf} \frac{(\gamma_L + d_L)\left(1 - \Sigma_\rho \Delta t / \Sigma_y\right) - d_U}{\Delta t \sqrt{2\Sigma_c}} \right) d\gamma_L \\
= &\int_{-\infty}^{0} \frac{1}{n} N(\gamma_L + d_L : 0, \Sigma_\gamma) \\
&\times \left[\frac{d}{dz_1} \frac{1}{2} \left(\text{erf} \frac{z_1}{\sqrt{2}} - \text{erf} \frac{z_2}{\sqrt{2}} \right) \frac{dz_1}{dt} \right. \\
&\left. + \frac{d}{dz_2} \frac{1}{2} \left(\text{erf} \frac{z_1}{\sqrt{2}} - \text{erf} \frac{z_2}{\sqrt{2}} \right) \frac{dz_2}{dt} \right] d\gamma_L \\
= &\int_{-\infty}^{0} \frac{1}{n} N(\gamma_L + d_L : 0, \Sigma_\gamma) \\
&\times \left[N(z_1 : 0, 1) \frac{dz_1}{dt} - N(z_2 : 0, 1) \frac{dz_2}{dt} \right] d\gamma_L
\end{aligned}
\tag{26}
$$

where

$$z_1 \equiv \frac{(\gamma_L + d_L)\left(1 - \Sigma_\rho \Delta t / \Sigma_y\right) - d_L}{\Delta t \sqrt{\Sigma_c}}$$

$$\approx \frac{\gamma_L - h_L \Delta t}{\Delta t \sqrt{\Sigma_c}}, \tag{27}$$

$$z_2 \equiv \frac{(\gamma_L + d_L)\left(1 - \Sigma_\rho \Delta t / \Sigma_y\right) - d_U}{\Delta t \sqrt{\Sigma_c}}$$

$$\approx \frac{\gamma_L - (d_U - d_L)}{\Delta t \sqrt{\Sigma_c}}, \tag{28}$$

and

$$\frac{dz_1}{dt} = -\frac{\gamma_L}{\Delta t^2 \sqrt{\Sigma_c}} \tag{29}$$

$$\frac{dz_2}{dt} = -\frac{\gamma_L - (d_U - d_L)}{\Delta t^2 \sqrt{\Sigma_c}}. \tag{30}$$

The leading functions $N()/n$ in the integrand of Eqn. (26) are smooth, but the others (in the square brackets) are not. These terms are expanded as

$$
\begin{aligned}
[\cdot] &= \left[-\frac{\gamma_L}{\Delta t^2 \sqrt{\Sigma_c}} N\left(\frac{\gamma_L - h_L \Delta t}{\Delta t \sqrt{\Sigma_c}} : 0, 1\right) \right. \\
&\quad \left. + \frac{\gamma_L - (d_U - d_L)}{\Delta t^2 \sqrt{\Sigma_c}} N\left(\frac{\gamma_L - (d_U - d_L)}{\Delta t \sqrt{\Sigma_c}} : 0, 1\right) \right] \\
&= \left[-\frac{\gamma_L}{\Delta t} N\left(\gamma_L : h_L \Delta t, \Sigma_c \Delta t^2\right) \right. \\
&\quad \left. + \frac{\gamma_L - (d_U - d_L)}{\Delta t} N\left(\gamma_L : d_U - d_L, \Sigma_c \Delta t^2\right) \right]
\end{aligned} \tag{31}
$$

The first of these two terms is clearly approaching a delta function as $\gamma_L = 0$ with decreasing Δt, while the second has no bearing for the integral, because we only integrate up to $\gamma_L = 0$. To characterize the volume of the delta function, we take note of the following identity and its associated definite integral,

$$\int x N(x : a, A)\, dx = -A\, N(x : a, A) + \frac{a}{2} \operatorname{erf}\left(\frac{x - a}{\sqrt{2A}}\right)$$

$$\int_{-\infty}^0 x N(x : a, A)\, dx = -A N(a : 0, A) + a E_2(a : 0, A), \tag{32}$$

and compute the area under the delta function in the domain:

$$\int_{-\infty}^{0} -\frac{\gamma_L}{\Delta t} N\left(\gamma_L : h_L \Delta t, \Sigma_c \Delta t^2\right) d\gamma_L$$

$$= -\frac{1}{\Delta t} \left[-\Sigma_c \Delta t^2 N\left(h_L \Delta t : 0, \Sigma_c \Delta t^2\right) \right.$$

$$\left. + h_L \Delta t \, E_2\left(h_L \Delta t : 0, \Sigma_c \Delta t^2\right) \right]$$

$$= \Sigma_c N(h_L : 0, \Sigma_c) - h_L \, E_2(h_L : 0, \Sigma_c). \tag{33}$$

Using the sifting property of the delta function, the integral in Eqn. (26) is equal to the value of the integrand evaluated at $\gamma_L = 0$ multiplied by the area in Eqn. (33), resulting in

$$C_3 = \frac{1}{n_0} N(d_L : 0, \Sigma_y)$$

$$\times \left(\Sigma_c N(h_L : 0, \Sigma_c) - h_L E_2(h_L : 0, \Sigma_c) \right). \tag{34}$$

C_4 is obtained through a parallel derivation, with the delta function appearing at d_U rather than d_L.

4 Conclusions

We have derived a single differential equation that completely encodes the boundaries in a time-varying, linear first-excursion problem. This formulation is made possible by a truncated Gaussian approximation, which holds reasonably for the damping ratios usually employed in closed-look systems, and over satisfactory time scales. The approach is computationally attractive for several examples considered, wherein a dynamic agent under closed-loop control is forced by stochastic noise. Thus, it lends itself to on-line path planning in a stochastic environment.

References

[1] Harris, S., 1981. "Steady, one-dimensional brownian motion with an absorbing boundary". *Journal of Chemical Physics,* **75**(6), pp. 3103–3106.

[2] Montroll, E. W., and Scher, H., 1973. "Random walks on lattices: Continuous-time walks and influence of absorbing boundaries". *Journal of Statistical Physics,* **9**(2), pp. 101–135.

[3] Bach, E., Coppersmith, S., Goldschen, M. P., Joynt, R., and Watrous, J., 2004. "One-dimensional quantum walks with absorbing boundaries". *Journal of Computer and System Sciences,* **69**(4), pp. 562–592.

[4] Burkhardt, T. W., 2002. "Absorption of a randomly accelerated particle: Recent results for partially absorbing and inelastic boundaries". *Physica A: Statistical Mechanics and its Applications,* **306**, pp. 107–116.

[5] Crandall, S., 1970. "First-crossing probabilities of the linear oscillator". *Journal of Sound and Vibration,* **12**(3), pp. 285–299.

[6] Vanmarcke, E., 1975. "Distribution of first-passage time for normal stationary random processes". *Journal of Applied Mechanics,* **42**(1), pp. 215–220.

[7] Langley, R., 1988. "A first passage approximation for normal stationary random processes". *Journal of Sound and Vibration,* **122**(2), pp. 261–275.

[8] Lin, Y., and Cai, G., 2004. *Probabilistic Structural Mechanics*. McGraw-Hill.

[9] He, J., 2009. "Numerical calculation for first excursion probabilities for linear systems". *Probabilistic Engineering Mechanics,* **24**, pp. 418–425.

[10] Au, S., and Beck, J., 2001. "First excursion probabilities for linear systems by very efficient importance sampling". *Probabilistic Engineering Mechanics,* **16**, pp. 193–207.

[11] Erdmann, M., 1985. "Using backprojections for fine motion planning with uncertainty". *Proceedings of the 1985 IEEE International Conference on Robotics and Automation*, Vol. 2, pp. 549–554.

[12] Blackmore, L., 2006. "A probabilistic particle control approach to optimal, robust predictive control". *Proceedings of the AIAA Guidance, Navigation and Control Conference*.

[13] Roy, N., and Thrun, S., 1999. "Coastal navigation with mobile robots". *Advances in Neural Processing Systems,* **12**, pp. 1043–1049.

[14] Greytak, M., and Hover, F., 2009. "Motion planning with an analytic risk cost for holonomic vehicles". *Proceedings of the 2009 IEEE Conference on Decision and Control*, pp. 5655–5660.

[15] Hockenberry, J., and Lesieutre, B., 2004. "Evaluation of uncertainty in dynamic simulations of power system models: The probabilistic collocation method". *IEEE Transactions on Power Systems,* **19**(3), pp. 1483–1491.